Silicon Photonics Design, Fabrication & Data Analysis of a Mach-Zehnder Interferometer

Tamzin Ellis

***Abstract*—This course report documents the design, fabrication and data analysis of Mach-Zehnder interferometer (MZI) structures on a photonic integrated circuit using strip waveguides on silicon-on-insulator (SOI) platform. Designs were made with variations in the a) fundamental polarisation (TE, transverse electric; TM, transverse magnetic) and b) waveguide length mismatch between arms of the interferometer. We will compare results of the extracted waveguide group index values from simulations to experimental data, considering manufacturing variabilities.**

***Index Terms*—Silicon photonics, Mach-Zehnder interferometer, free spectral range.**

I. Introduction

THIS course report documents the fundamental theory behind MZIs in Section II, the designs of our MZI structures and simulated results in Section III, and details of fabrication in Section IV. Sections IV and V detail the experimental data and analysis, respectively. Finally, we conclude in Section VII.

II. Theory

The Mach-Zehnder interferometer consists of an input split into two branches, which are recombined to form one or two outputs. The splitting and combining can be achieved using, for example, Y-branches, directional couplers, and adiabatic couplers. A simple model based on the plane-wave free-space beamsplitter can be used to describe the total field intensities within each waveguide [1]. For the interferometer using Y-branches as splitters, let the input intensity be I_i with corresponding electric field E_i. At the output of the splitter Y-branch, the top and bottom branches have electric field E_1 and E_2, respectively, with both $E_1 = E_2 = E_i/\sqrt{2}$. The lengths of the waveguides are L_1 and L_2 with propagation constants $\beta_1 = 2\pi n_1/\lambda$ and $\beta_2 = 2\pi n_2/\lambda$ (where $n_{1,2}$ are effective indices and λ is the optical wavelength), and propagation loss $\alpha_1/2$ and $\alpha_2/2$ for the top and bottom branches, respectively. At the input to the combiner Y-branch the electric fields are:

$$E_{o1} = E_1 e^{-i\beta_1 L_1 - \frac{\alpha_1}{2}L_1} = \frac{E_i}{\sqrt{2}} e^{-i\beta_1 L_1 - \frac{\alpha_1}{2}L_1} \tag{1}$$

$$E_{o2} = E_2 e^{-i\beta_2 L_2 - \frac{\alpha_2}{2}L_2} = \frac{E_i}{\sqrt{2}} e^{-i\beta_2 L_2 - \frac{\alpha_2}{2}L_2} \tag{2}$$

At the output of the combiner Y-branch, the electric field is:

$$E_o = \frac{1}{\sqrt{2}}(E_{o1} + E_{o2}) = \frac{E_i}{2}(e^{-i\beta_1 L_1 - \frac{\alpha_1}{2}L_1} + e^{-i\beta_2 L_2 - \frac{\alpha_2}{2}L_2}) \tag{3}$$

Since intensity $I \propto |E^2|$, the intensity at the output is thus:

$$I_o = \frac{I_i}{4}|e^{-i\beta_1 L_1 - \frac{\alpha_1}{2}L_1} + e^{-i\beta_2 L_2 - \frac{\alpha_2}{2}L_2}| \tag{4}$$

Assuming that the total losses are negligible and both arms of the interferometer have the same propagation constant $\beta = \beta_1 = \beta_2$ (i.e., are identical to one another, excluding length), the output intensity simplifies to:

$$I_o = \frac{I_i}{2}[1 + \cos(\beta \Delta L)], \tag{5}$$

where $\Delta L = L_1 - L_2$ is the path length imbalance between the arms. This is called an optical transfer function, which varies sinusoidally with wavelength with a period equal to the Free Spectral Range (FSR) of the interferometer. The FSR is determined by the following expression:

$$\text{FSR} = \frac{\lambda^2}{n_g \Delta L}, \tag{6}$$

where n_g is the waveguide group index. Therefore, through the FSR parameter, the sinusoidal oscillation seen in the Mach-Zehnder interferometer spectrum allows for the extraction of the waveguide group index.

Additionally, a compact model for the waveguide effective index can be found in the form of a second-order polynomial in wavelength λ. A Taylor expansion around the centre wavelength λ_0 can be used to derive a compact model of the form:

$$n_{\text{eff}}(\lambda) = n_1 + n_2(\lambda - \lambda_0) + n_3(\lambda - \lambda_0)^2, \tag{7}$$

where n_1, n_2 and n_3 can be converted to conventional parameters at the centre wavelength λ_0: effective index $n_{\text{eff}} = n_1$, group index $n_g = n_1 - n_2\lambda_0$ and dispersion $D = -2\lambda_0 n_3/c$.

III. Modelling and simulation

A. The waveguide

The optical waveguide is a strip waveguide with a silicon core of height 220 nm and width 500 nm surrounded by silicon dioxide cladding. Firstly, the fundamental TE and TM modes are simulated using Lumerical Finite-difference Eigenmode Solver (FDE). The results are plotted for the dominant field profiles for each mode in Figure 1. Note, the fundamental TE mode is in fact quasi-TE polarised with a TE polarisation fraction of 99%, and the fundamental TM mode is quasi-TM polarised with a TE polarisation fraction of 4%.

The compact model for the waveguide is derived using curve fitting in Lumerical FDE. After performing a wavelength sweep between 1500 nm and 1600 nm of the effective index,

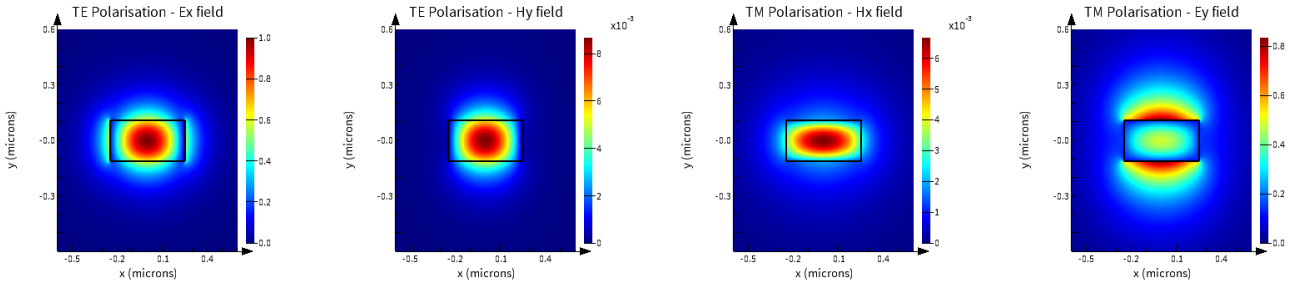

(a) (b) (c) (d)

Fig. 1: Simulated results for the dominant fields of the mode profile of the fundamental (quasi-)TE mode, (a) and (b), and the fundamental (quasi-)TM mode, (c) and (d).

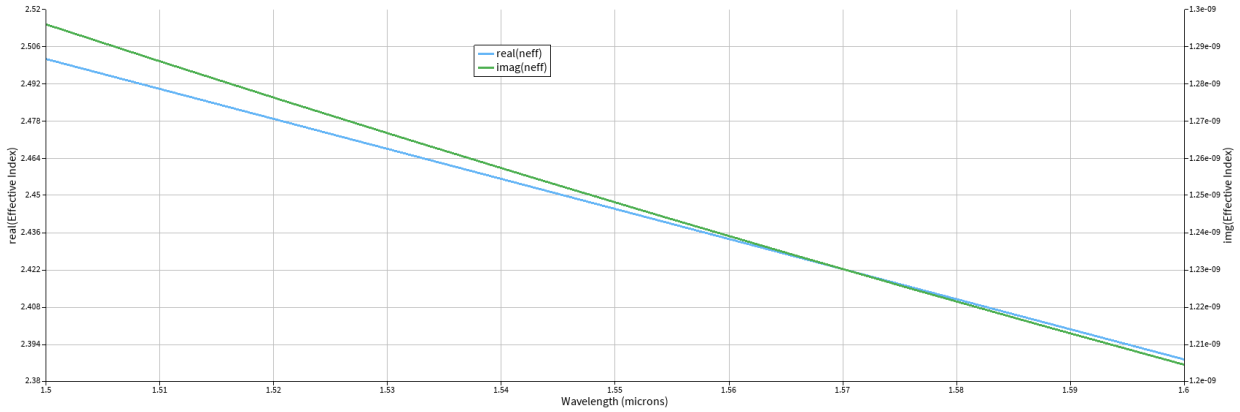

Fig. 2: The waveguide effective refractive index versus wavelength. The real part is shown in light blue and uses the left axis, and the imaginary part is shown in green and uses the right axis.

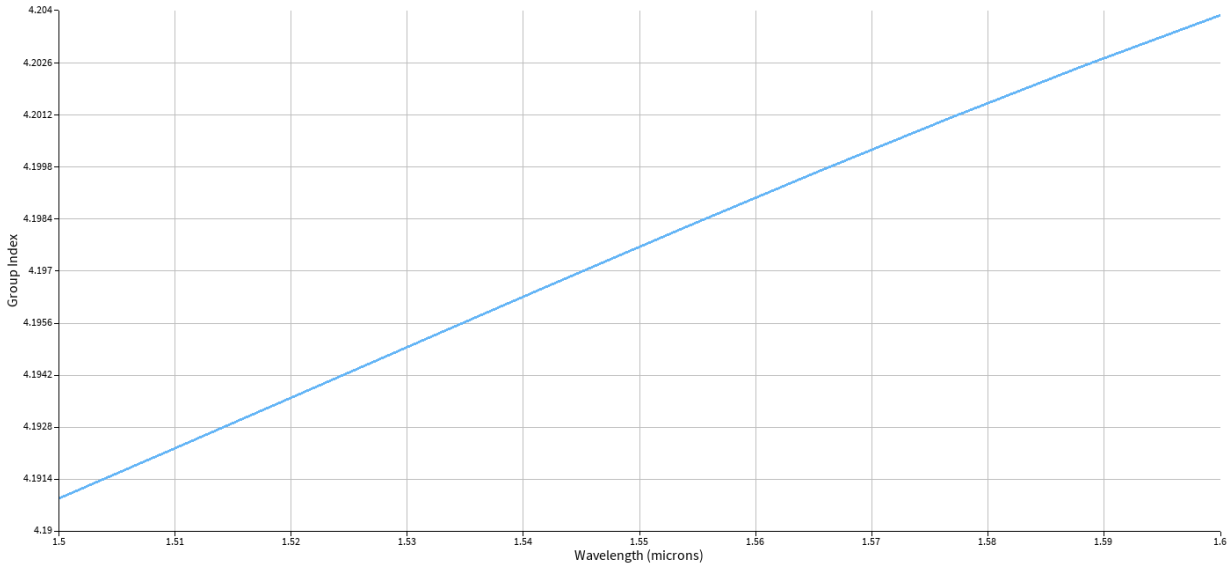

Fig. 3: The waveguide group index versus wavelength.

TABLE I: Compact model

Parameter	Value
n_1	2.44487
n_2	-1.13077
n_3	-0.0424695

TABLE II: Variation of FSR with path length difference

Path length difference ΔL (m)	FSR (nm) of peak closest to 1550 nm
50	11.43
100	5.62
150	3.77
200	2.84
250	2.30

a MATLAB script is used to fit a second-order polynomial to the data, returning the coefficients n_1, n_2 and n_3 given in Table I. Thus, the model is given by the following expression:

$$n_{\text{eff}}(\lambda) = 2.445 - 1.131(\lambda - \lambda_0) - 0.042(\lambda - \lambda_0)^2. \quad (8)$$

Figure 2 and Figure 3 shows the simulated results for the wavelength sweep of the waveguide effective index and group index, respectively.

B. The Mach-Zehnder interferometer

The Mach-Zehnder interferometer circuit consisting of a Y-branch splitter and Y-branch combiner connected to an Optical Network Analyser is shown in Figure 4. The circuit is simulated in Lumerical INTERCONNECT using the SiEPIC-EBeam-PDK Compact Model Library. In order to extract the FSR from simulations, the interferometer must be imbalanced, i.e., have a path length difference between the arms. Since the path length difference needs to be greater than 30 μm to see a least one FSR in the 50 μm bandwidth limited by the grating couplers, we use path length variations from 25 μm to 200 μm.

The layout of the four MZIs plus a grating coupler loopback de-embedding structure for each fundamental polarisation mode is shown in Figure 5. KLayout was used to draw the mask layout with the Si-EPIC-EBeam-PDK Compact Model Library components. Figure 6 and Figure 7 show the transmission spectra for the MZIs designed for the fundamental TE mode and fundamental TM mode, respectively. Additionally, simulation results for the FSR of the peak nearest 1550 nm for each path length difference is shown in Table II. It is evident that the FSR decreases as the path length imbalance increases, as expected from Equation (6).

IV. Fabrication

Fabricated is performed at one or more of these: Applied Nanotools and Washington Nanofabrication Facility. The following are the process descriptions.

Applied Nanotools, Inc. NanoSOI process: The photonic devices were fabricated using the NanoSOI MPW fabrication process by Applied Nanotools Inc. (http://www.appliednt.com/nanosoi; Edmonton, Canada) which is based on direct-write 100 keV electron beam lithography technology. Silicon-on-insulator wafers of 200 mm diameter, 220 nm device thickness and 2 μm buffer oxide thickness are used as the base material for the fabrication. The wafer was pre-diced into square substrates with dimensions of 25x25 mm, and lines were scribed into the substrate backsides to facilitate easy separation into smaller chips once fabrication was complete. After an initial wafer clean using piranha solution (3:1 H2SO4:H2O2) for 15 minutes and water/IPA rinse, hydrogen silsesquioxane (HSQ) resist was spin-coated onto the substrate and heated to evaporate the solvent. The photonic devices were patterned using a JEOL JBX-8100FS electron beam instrument at The University of British Columbia. The exposure dosage of the design was corrected for proximity effects that result from the backscatter of electrons from exposure of nearby features. Shape writing order was optimized for efficient patterning and minimal beam drift. After the e-beam exposure and subsequent development with a tetramethylammonium sulfate (TMAH) solution, the devices were inspected optically for residues and/or defects. The chips were then mounted on a 4" handle wafer and underwent an anisotropic ICP-RIE etch process using chlorine after qualification of the etch rate. The resist was removed from the surface of the devices using a 10:1 buffer oxide wet etch, and the devices were inspected using a scanning electron microscope (SEM) to verify patterning and etch quality. A 2.2 μm oxide cladding was deposited using a plasma-enhanced chemical vapour deposition (PECVD) process based on tetraethyl orthosilicate (TEOS) at 300ºC. Reflectrometry measurements were performed throughout the process to verify the device layer, buffer oxide and cladding thicknesses before delivery.

Washington Nanofabrication Facility (WNF) silicon photonics process The devices were fabricated using 100 keV Electron Beam Lithography [2]. The fabrication used silicon-on-insulator wafer with 220 nm thick silicon on 3 μm thick silicon dioxide. The substrates were 25 mm squares diced from 150 mm wafers. After a solvent rinse and hot-plate dehydration bake, hydrogen silsesquioxane resist (HSQ, Dow-Corning XP-1541-006) was spin-coated at 4000 rpm, then hotplate baked at 80 °C for 4 minutes. Electron beam lithography was performed using a JEOL JBX-6300FS system operated at 100 keV energy, 8 nA beam current, and 500 μm exposure field size. The machine grid used for shape placement was 1 nm, while the beam stepping grid, the spacing between dwell points during the shape writing, was 6 nm. An exposure dose of 2800 μC/cm2 was used. The resist was developed by immersion in 25% tetramethylammonium hydroxide for 4 minutes, followed by a flowing deionized water rinse for 60 s, an isopropanol

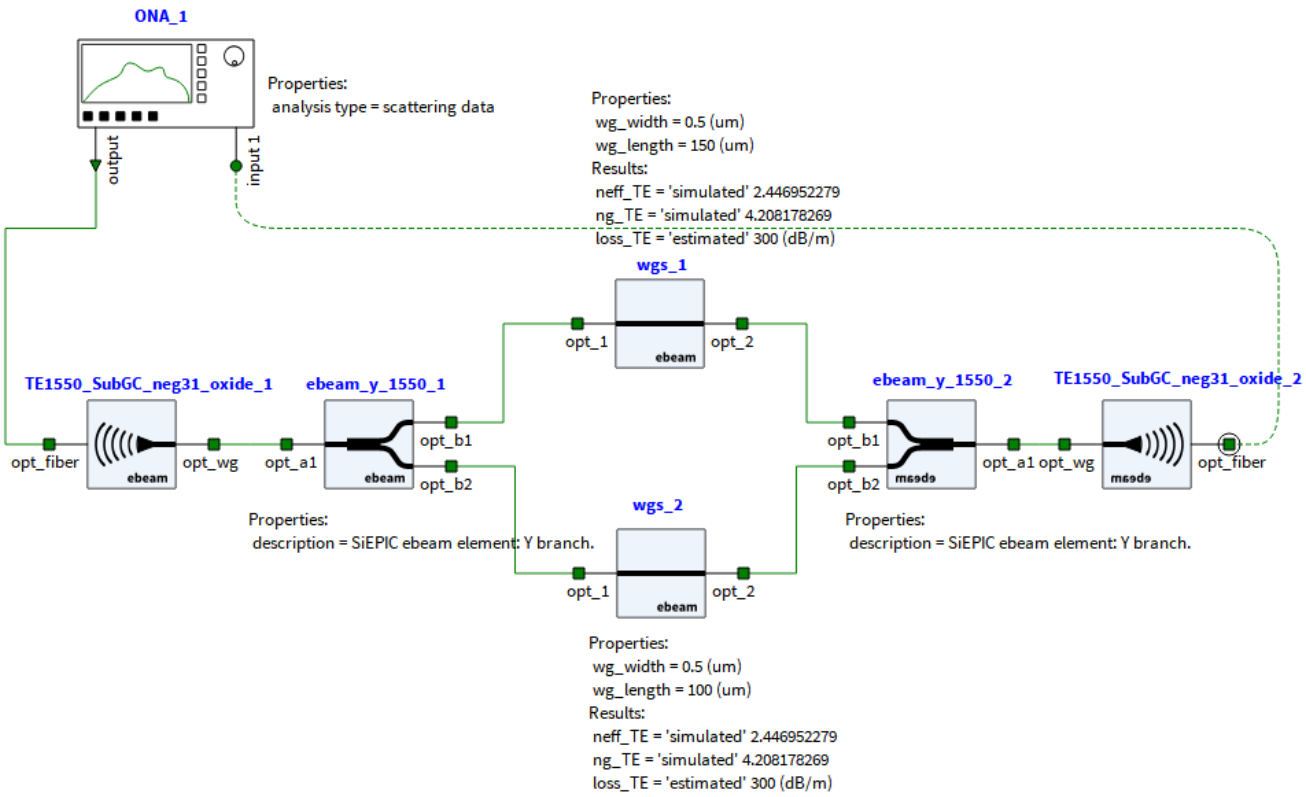

Fig. 4: The Mach-Zehnder interferometer circuit in Lumerical INTERCONNECT. Grating couplers and waveguides are designed for the fundamental (quasi-)TE mode and a wavelength of 1550 nm.

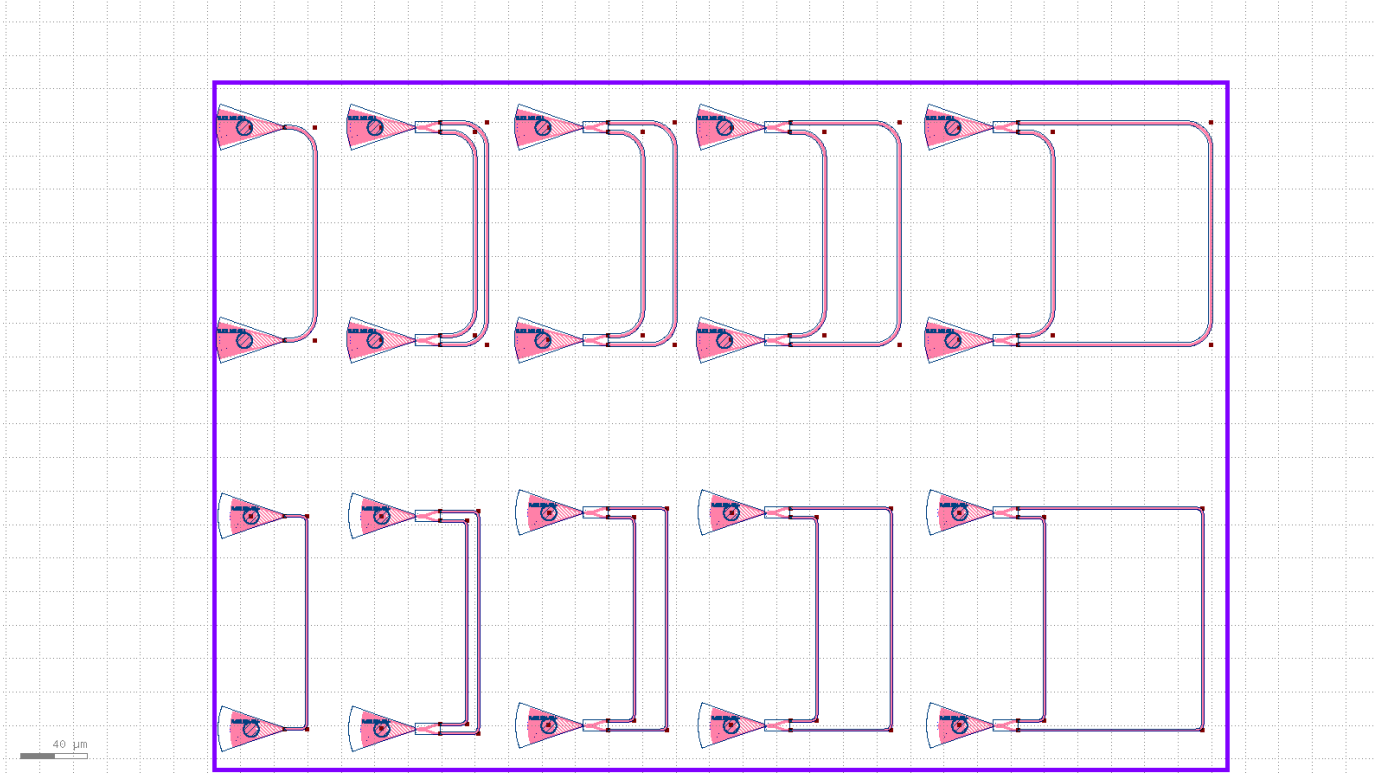

Fig. 5: The mask layout of the four MZIs plus a grating coupler loopback de-embedding structure for each fundamental polarisation mode designed in KLayout. The top (bottom) structures are designed for the fundamental TM (TE) mode.

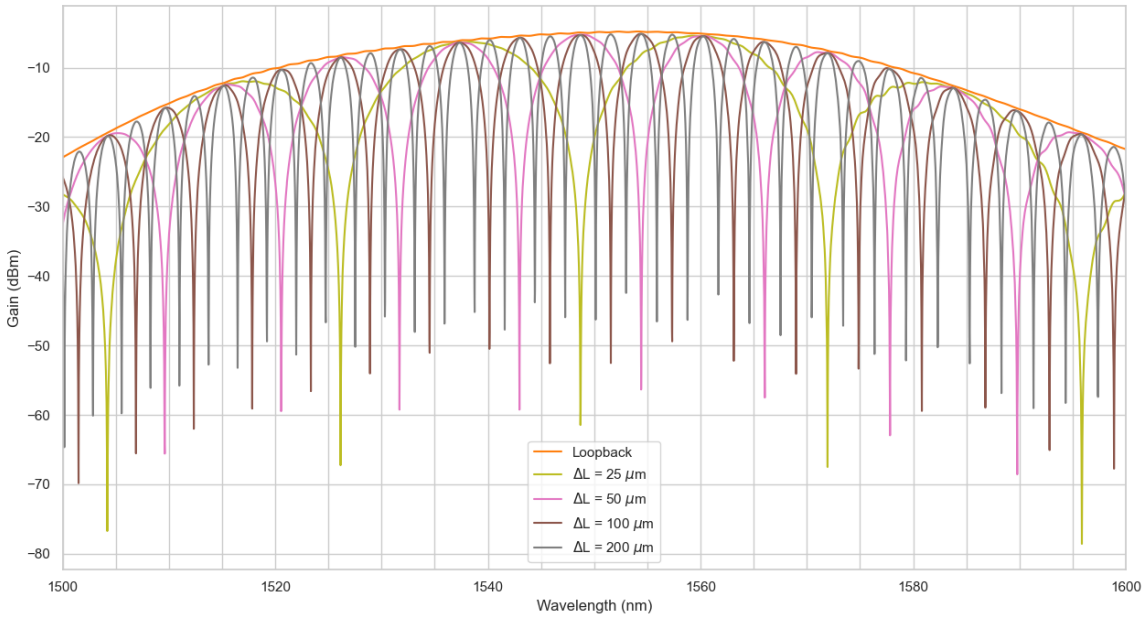

Fig. 6: The simulated transmission spectrum for the Mach-Zehnder interferometer circuit designed for the fundamental TE mode, for four variations of path length imbalance, $\Delta L = 25, 50, 100, 200$ μm, and a grating coupler loopback de-embedding structure. The FSR decreases with increasing path length imbalance, as expected.

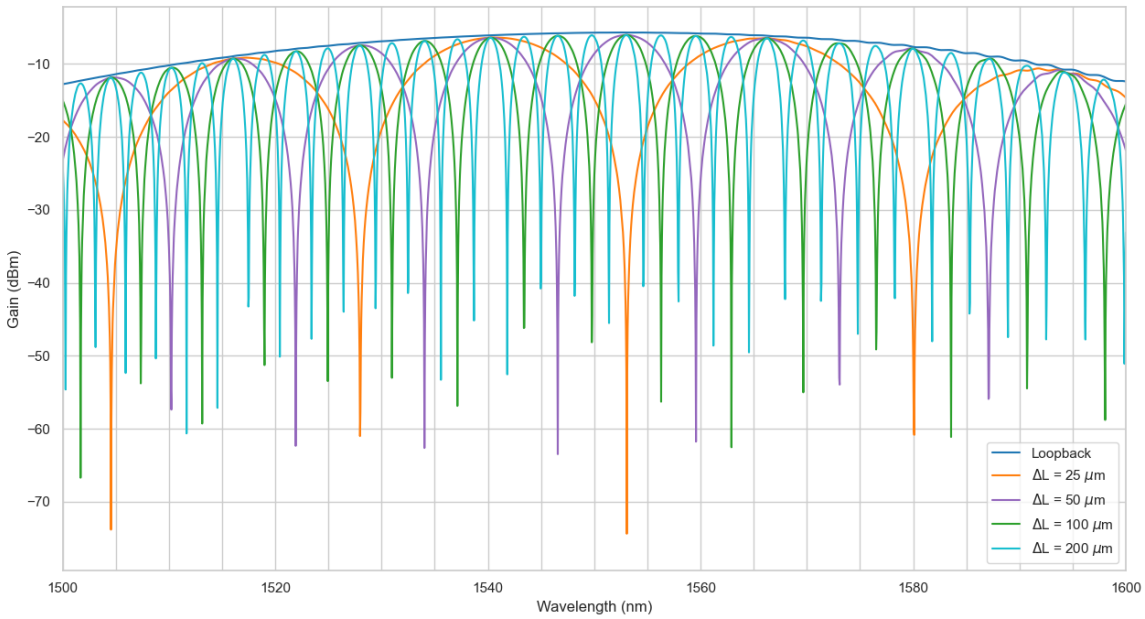

Fig. 7: The simulated transmission spectrum for the Mach-Zehnder interferometer circuit designed for the fundamental TM mode, for four variations of path length imbalance, $\Delta L = 25, 50, 100, 200$ μm, and a grating coupler loopback de-embedding structure.

rinse for 10 s, and then blown dry with nitrogen. The silicon was removed from unexposed areas using inductively coupled plasma etching in an Oxford Plasmalab System 100, with a chlorine gas flow of 20 sccm, pressure of 12 mT, ICP power of 800 W, bias power of 40 W, and a platen temperature of 20 °C, resulting in a bias voltage of 185 V. During etching, chips were mounted on a 100 mm silicon carrier wafer using perfluoropolyether vacuum oil. Cladding oxide was deposited using plasma enhanced chemical vapor deposition (PECVD) in an Oxford Plasmalab System 100 with a silane (SiH4) flow of 13.0 sccm, nitrous oxide (N2O) flow of 1000.0 sccm, high-purity nitrogen (N2) flow of 500.0 sccm, pressure at 1400mT, high-frequency RF power of 120W, and a platen temperature of 350C. During deposition, chips rest directly on a silicon carrier wafer and are buffered by silicon pieces on all sides to aid uniformity.

V. Experiment Data

To characterize the devices, a custom-built automated test setup [1], [6] with automated control software written in Python was used [3]. An Agilent 81600B tunable laser was used as the input source and Agilent 81635A optical power sensors as the output detectors. The wavelength was swept from 1500 to 1600 nm in 10 pm steps. A polarization maintaining (PM) fibre was used to maintain the polarization state of the light, to couple the TE polarization into the grating couplers [4]. A 90º rotation was used to inject light into the TM grating couplers [4]. A polarization maintaining fibre array was used to couple light in/out of the chip [5].

VI. Analysis

For our analysis of our experimental results, we curve-fit the analytical expression for the transfer function to the experimental transmission spectra using the least-squares method in MATLAB. The objective of this is to extract the waveguide parameters, namely the group index and the dispersion. We use the function `findpeaks` to locate the minima of the spectra, allowing the determination of the free spectral range and thus the group index via Equation 6. Figures 8 to 13 show the steps for extracting the group index and dispersion from the transmission spectra. The extracted parameters for this particular MZI (path length mismatch 200 µm, TE mode) are group index 4.188 and dispersion 534.0023 ps/nm/km at a wavelength of 1.5354 µm.

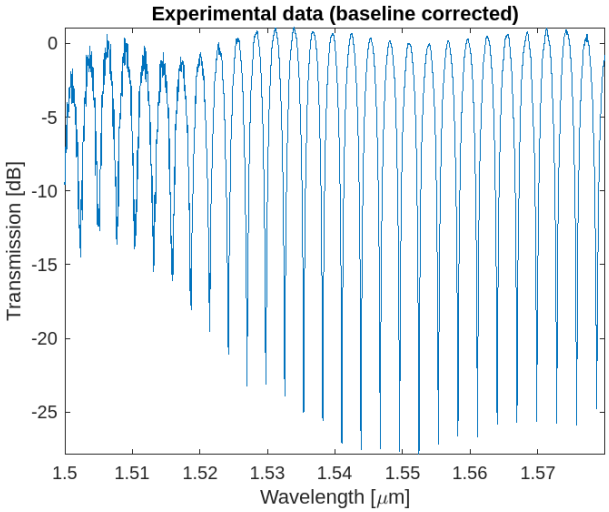

Fig. 8: Experimental data with baseline correction applied to remove the effect of grating coupler insertion loss.

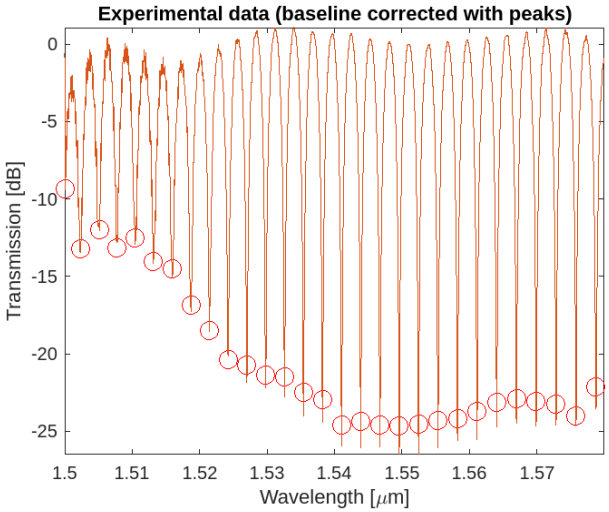

Fig. 9: Experimental data with baseline correction highlighting the peaks of the spectra.

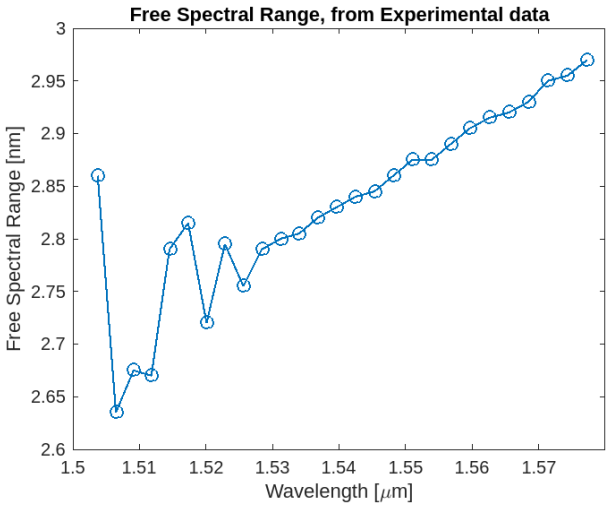

Fig. 10: The free spectral range extracted from Fig. 9.

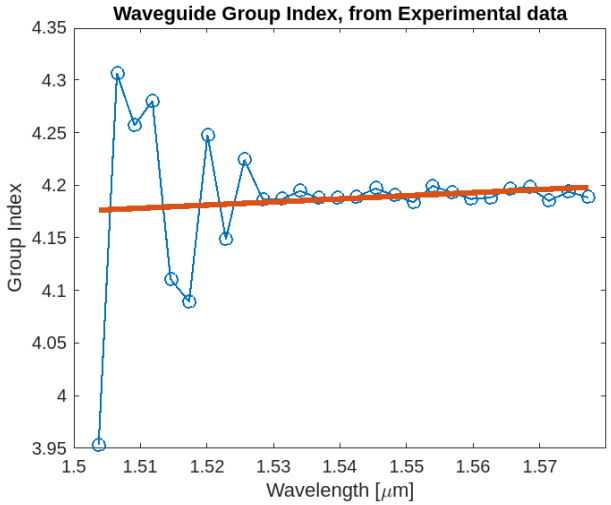

Fig. 11: The MZI transfer function fit (orange) to the data using inital parameters.

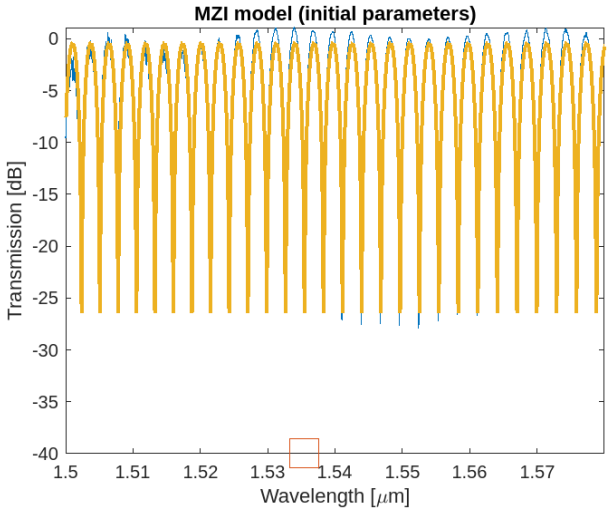

Fig. 12: The waveguide group index with wavelength. Large fluctuations even out after a wavelength of around 1.53 µm.

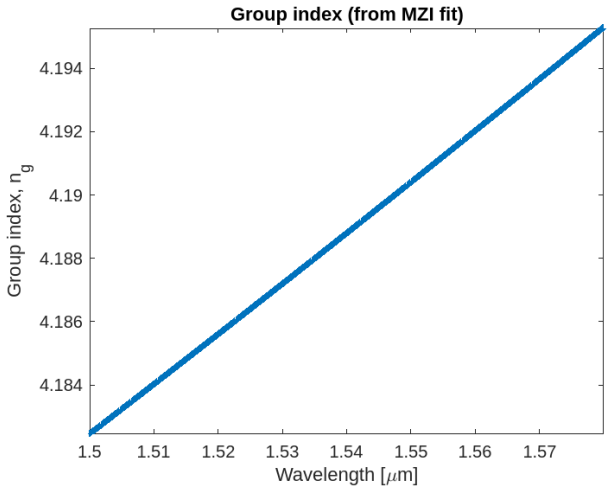

Fig. 14: Group index from the MZI transfer function with wavelength.

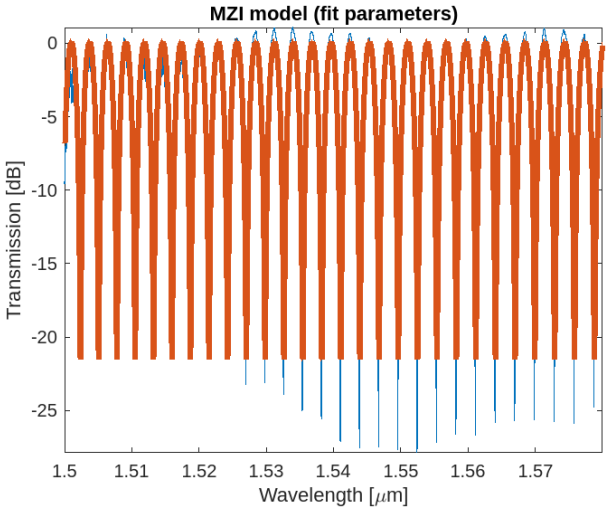

Fig. 13: The MZI transfer function (red) fit to the experimental data showing a good fit with goodness of fit value 0.94588.

VII. Conclusion

MZIs with path length imbalances were designed, fabricated and tested to compare experimental results to simulations.

Acknowledgements

I acknowledge the edX UBCx Phot1x Silicon Photonics Design, Fabrication and Data Analysis course, which is supported by the Natural Sciences and Engineering Research Council of Canada (NSERC) Silicon Electronic-Photonic Integrated Circuits (SiEPIC) Program. I also acknowledge Lumerical Solutions, Inc., Mathworks, Mentor Graphics, Python, and KLayout for the design software.

References

[1] Chrostowski, L., & Hochberg, M. (2015). *Silicon photonics design: from devices to systems.* Cambridge University Press.
[2] R. J. Bojko, J. Li, L. He, T. Baehr-Jones, M. Hochberg, & Y. Aida, “Electron beam lithography writing strategies for low loss, high confinement silicon optical waveguides,” J. Vacuum Sci. Technol. B 29, 06F309 (2011)
[3] http://siepic.ubc.ca/probestation, using Python code developed by Michael Caverley.
[4] Yun Wang, Xu Wang, Jonas Flueckiger, Han Yun, Wei Shi, Richard Bojko, Nicolas A. F. Jaeger, Lukas Chrostowski, ”Focusing sub-wavelength grating couplers with low back reflections for rapid prototyping of silicon photonic circuits”, Optics Express Vol. 22, Issue 17, pp. 20652-20662 (2014)
[5] www.plcconnections.com, PLC Connections, Columbus OH, USA.
[6] http://mapleleafphotonics.com, Maple Leaf Photonics, Seattle WA, USA.